ARTICLES

Theoretical Study on Magnetostructural Correlation in Unsymmetrical Oxamidocopper(II) Complexes

Siwei Bi,[†,‡] Chengbu Liu,*[,†] and Haiquan Hu[†]

Institute of Theoretical Chemistry, Shandong University, Shandong, Jinan 250100, People's Republic of China, and Department of Chemistry, Qufu Normal University, Shandong, Qufu 273165, People's Republic of China

Received: January 16, 2002; In Final Form: April 9, 2002

The theoretical study on magnetostructural correlation in unsymmetrical Cu(II) binuclear complexes bridged by $[C_2O_2(NH)_2]^{2-}$ has been performed using the broken symmetry approach within the framework of density functional theory (DFT). The calculated results show that the magnetic coupling interaction decreases with the changes of the coordination environment around the Cu atom from a planar structure, via an intermediate environment between a trigonal bipyramid and a square pyramid, to a square pyramid. The magnetostructural correlation is explored in detail through the variation of the coordination environments by changing bond angles. The calculated results indicate that the magnetic coupling constant J is linearly related to bond angle θ, the spin populations ρ on Cu atoms, and the square of the difference in energy of the unpaired electrons $(\epsilon_1 - \epsilon_2)^2$, respectively, when the bonding energy decreases with the variation of the coordination environments. However, the deviation from the linear relationship appears as the bonding energy increases. Another parameter, the difference of the squared spin populations on Cu atoms between the triplet and the broken states ($\rho_T^2 - \rho_{BS}^2$), is found having an approximately linear relationship to J whether the bonding energy decreases or increases. So it may be more suitable than $(\epsilon_1 - \epsilon_2)^2$ in describing the linear relationship to J and extended to some other binuclear Cu(II) systems for the investigation of magnetostructural correlations.

Introduction

The theoretical study on the magnetic behavior of polynuclear metal complexes represents a great challenge due to the existence of a manifold of states separated by small energy difference. The study on the magnetostructural correlation of polynuclear systems has drawn much attention in recent years for elucidating magnetic phenomena, designing new molecular magnetic materials, and investigating the role of the polymetallic active sites in biological processes.[1−6] Many theoretical investigations on magnetostructural correlation have been carried out for such binuclear Cu(II) systems[7−21] as those bridged by −OH, $-OCH_3$, and N_3^- groups, in which the Cu(II) ions in each compound have idenical coordination environments. As pointed out elsewhere,[7−14] there are many factors affecting magnetic behaviors, such as bond angles, the trans or cis structures of bridging groups, or the different coordination environments of magnetic centers. To some extent, the terminal groups serve as "adjusting screws" for tuning the magnitude of magnetic coupling interaction.

N,N′-disubstituted oxamides are versatile ligands for the design and preparation of polynuclear systems. In this paper, we devote mainly to the magnetic coupling interaction and the magnetostructural correlation for *cis*-oxamido-bridged binuclear Cu(II) complexes, where Cu(II) ions have different coordination environments. The aim of this work is, on one hand, to discuss the magnetic coupling interaction of the compounds with different coordination geometries and, on the other hand, to analyze the magnetostructural correlation in this system.

The presence of low-energy singlet states near the lowest singlet state makes the evaluation of the energy of binuclear Cu(II) complexes difficult within a monodeterminant method. To solve this problem, the broken symmetry approach put forward by Noodleman[22] is employed here to investigate the magnetic coupling interaction of the present complexes. In this work, the broken symmetry approach combined with the density functional theory (DFT) is used to explore the magnetic coupling interaction and the magnetostructural correlation for Cu(II) binuclear systems. The paper is organized as follows: The next part deals with the calculation details. The following part describes the model complexes and then presents the calculation results and discussion. The conclusions are given in the last part.

Computational Details

For Cu(II) binuclear systems, using $\hat{H} = -2J\hat{S}_1 \cdot \hat{S}_2$, we evaluate the magnetic coupling constant J by the following equation:[23]

$$E_T - E_S = -2J \tag{1}$$

where E_T and E_S denote the energies of triplet and singlet states,

[†] Shandong University.
[‡] Qufu Normal University.

10.1021/jp0201276 CCC: $22.00
Published on Web 10/01/2002

respectively. Positive J value means ferromagnetic behavior, and negative one means antiferromagnetic behavior.

A qualitative approach having been employed successfully for the interpretation of magnetostructural correlation was developed by Hay et al.[23] For the case of Cu(II) dimers, a formula[23] was obtained as follows:

$$2J = 2K_{ab} - \frac{(\epsilon_1 - \epsilon_2)^2}{(J_{aa} - J_{bb})} \quad (2)$$

where ϵ_1 and ϵ_2 are the energies of the two highest singly occupied molecular orbitals in the triplet state, while K_{ab}, J_{aa}, and J_{bb} are two-electron integrals. Equation 2 is mainly employed to describe the linear relationship between the coupling constant J and $(\epsilon_1 - \epsilon_2)^2$, assuming that the two-electron terms are approximately constant for the same metal atoms and bridging ligands. However, as we will point out later in this paper, the linear relationship between J and $(\epsilon_1 - \epsilon_2)^2$ would not exist if the changes of geometrical configuration occur remarkably.

The broken symmetry approach within the framework of the density functional theory is efficient to calculate the coupling constant J within a monodeterminant. A single configuration representing the essential features of the resulting antiferromagnetic state is developed in this method. When magnetic orbitals are allowed to interact by overlapping in a self-consistent field (SCF) procedure, a state of mixed spin symmetry and lowered space symmetry, named as a mixed spin or broken symmetry state, is obtained. The energy of the mixed spin state is a specific weighted average of the energies of the pure spin multiplets. The broken symmetry wave function as a single determinant is not an eigenstate of $\hat{S}^2$ but corresponds to a total $M_s = 0$ state or, more generally, to the minimum M_s value. The Heisenberg exchange coupling constant J for binuclear systems can be determined from the energies of the mixed spin state and the highest spin multiplet state, as proposed by Noodleman.[22]

$$E(S_{max}) - E_{BS} = -{S_{max}}^2 J \quad (3)$$

For binuclear Cu(II) systems,

$$E_T - E_{BS} = -J \quad (4)$$

On the basis of eq 4, the Heisenberg exchange coupling constant J for Cu(II) dimers can be determined from the energies of the mixed spin state and the highest spin multiplet state. This method offers an approximation to a limited configuration interaction.

Many investigations of the magnetic behavior for polynuclear systems have been performed using eq 3. However, we find that the calculated J values are usually larger than the experimental ones within the framework of DFT.[7,10,24,25] As previously reported, local functionals overestimate the relative stabilization of the singlet state relative to the triplet state.[26] So, recently, the energy of the BS (broken symmetry) state was taken as an approximation to that of the pure singlet state in weak systems within the framework of DFT.[8,14] So eq 1 can be transformed into

$$E_T - E_{BS} = -2J \quad (5)$$

The choice of using either eq 4 or eq 5 has no major significance for the qualitative description of the magnetostructural correlations. In particular, the value of a structural parameter for which the crossover from ferro- to antiferromagnetic behavior occurs is independent of the approximation used to estimate the energy of the singlet state from that of the broken symmetry solution. In this paper, the BS state is employed to substitute the pure singlet state to calculate the coupling constant J of Cu(II) binuclear complexes by using eq 5.

Two methods have been employed for the calculations of magnetic constant J values. Method 1 (abbreviated as ADF-BS) uses the Amsterdam density functional (ADF) package (version 2.0.1). Vosko, Wilk, and Nusair's (VWN) functional is used for local spin density approximation (LSDA).[27] Generalized gradient correlations have been introduced by using the Becke exchange functional[28] and the Perdew correlation functional.[29] Triple-ζ basis sets extended with a polarization function are used for all atoms in the systems. The frozen core (FC) approximation for the inner core electrons is employed. The orbitals up to 2p for Cu and 1s for C, N, and O atoms are kept frozen. The scalar relativistic effect is taken into account.

Method 2 uses the Gaussian 98 package. Local spin density calculations have been carried out using the Slater exchange and Vosko, Wilk, and Nusair (VWN) correlation functionals. Generalized gradient correlations have been introduced using the Becke exchange part (B) and the Lee−Yang−Parr (LYP) correlation parts. The diabatic connection method using three parameters put forward by Becke (B3LYP), mixing the Hartree−Fock contribution for the exchange, has also been used. For evaluating the accuracy of other functionals used in density functional theory, the functionals such as SVWN, BLYP, B1LYP, and B3PW91 have also been tested. The basis set used in this method is standard 6-31G(d,p).

Model Complexes

In the analysis of the magnetostructural correlations, it is useful to employ model structures because the main aim in this case is to study the variation trend of magnetic behavior rather than just to compare the calculated J value with the experimental one. So model molecules are employed in this work to simplify calculations. The first experimental compound [Cu(oxpn)Cu(bpy)](ClO_4) (**i**)[30] has a planar structure (not including H atoms). There is an intermediate environment, between a trigonal bipyramid and a square pyramid, around one Cu(II) ion in the experimental compound Cu(oxpn)Cu(petdien)](ClO_4)$_2$ (**ii**) and a square pyramidal environment in [Cu(oxpn)Cu(pmedien)](ClO_4)$_2$ (**iii**).[30] Experimental results show that the magnetic coupling interaction in the three experimental compounds decreases in the order of **i**, **ii**, and **iii**.[30]

Models a and b are derived from the experimental compound **i**. Two H atoms link to the N atoms of $[C_2O_2(NH)_2]^{2-}$ in model a, and two methyl groups link to the N atoms of $[C_2O_2(NH)_2]^{2-}$ in model b. Models c and d are derived from the experimental compounds **ii** and **iii**. The bond lengths of models a, b, and c come from the corresponding experimental compounds. The bond lengths adopted in model d come from model c because the single crystal of the third experimental compound **iii** has not been prepared. The bond lengths of C−H and N−H bonds keep 1.08 and 1.01 Å, respectively.

As known to all, the framework of model b has a planar structure. The bridging network constituted by $[Cu_2C_2O_2(NH)_2]^{2+}$ is also made in a plane in the models a, c, and d (Figure 1), and the bond angles are very close to those of the experimental compounds. All of the terminal ligands are replaced by ammonia molecules. The frameworks of these models in Figure 1 do not include hydrogen atoms. Models a and b have planar structures, and models c and d have nonplanar

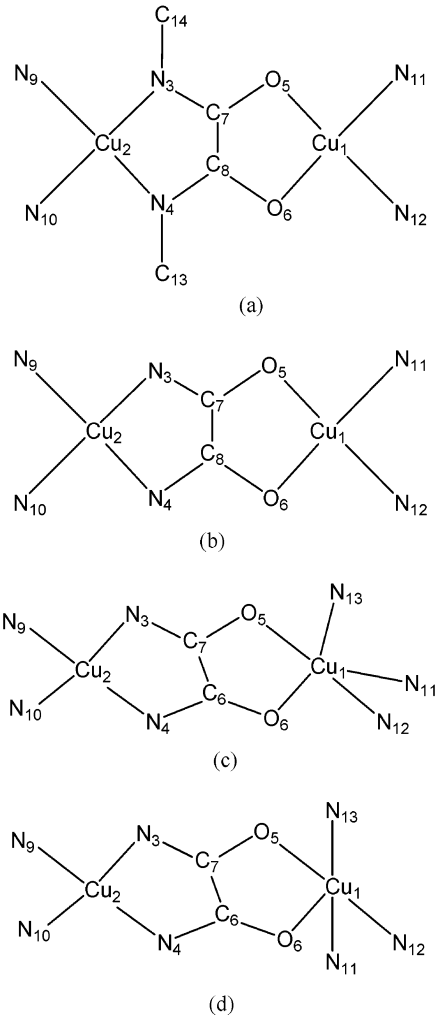

Figure 1. Structures of the models (not including H atoms).

TABLE 1: Calculated *J* Values (cm^{-1}) by Using Different Methods

	Gau-BS (method 2)					ADF−BS (method 1)
functional basis set:	SVWN 6-31G**	BLYP 6-31G**	B1LYP 6-31G**	B3LYP 6-31G**	B3PW91 6-31G**	VWN-BP triple-ζ
J(calcd)	−1736.0	−49062.3	−278.8	−358.12	−359.8	−787.1
J(exptl)			−439.7			

structures. As in the experimental compounds, the environment of the Cu1 atom in model c is in an environment intermediate between a trigonal bipyramid and a square pyramid. The Cu1 atom in model d is in a square pyramid environment. The plane in model d, constituted by O5, N13, N12, N11, and Cu1 atoms, is perpendicular to that of the bridging network, and O6 occupies the apical position of the square pyramid.

Results and Discussion

(1) Evaluation of Computational Accuracy with Different Functionals in DFT. With model b (Figure 1) selected as an example, the computational accuracy with method 1 and method 2 has been tested. Different functionals in method 2 are employed, such as SVWN, BLYP, B1LYP, B3LYP, and B3PW91. The calculated results are listed in Table 1.

For method 2, it can be seen from Table 1 that the functionals B3PW91 and B3LYP are more appropriate than the others. The *J* values calculated by using pure functionals are also usually larger than experimental data. In all of the following calculations, the functional B3LYP is adopted. For method 1, the calculated *J* value is larger than the experimental one, mainly due to the absence of hybrid parameters. As reported elsewhere,[7,10] however, the *J* values calculated by method 1 can well reflect the trend of magnetic coupling interaction with the variation of some structural parameters. Although method 1 is mainly employed to deal with the magnetostructural correlations, method 2 is also used to handle some relationships for the comparison to method 1.

TABLE 2: Magnetic Coupling Constants (cm^{-1}) and the Spin Populations on Cu1 and Cu2 Atoms

	model			
	a	b	c	d
$-J_1$(calcd)[a]	698.2	787.1	656.1	226.8
$-J_2$(calcd)[a]	398.2	439.7	290.6	98.9
$-J$(exptl)	439.7	439.7	242.2	82.8
ρ(Cu1)[b]	−0.4559	−0.4446	−0.4888	−0.4948
ρ(Cu2)[b]	0.4231	0.4208	0.4344	0.4563

[a] $-J_1$(calcd) and $-J_2$(calcd) are calculated by method 1 and method 2, respectively. [b] ρ(Cu1) and ρ(Cu2), calculated using method 1, denote the spin population on Cu1 and Cu2 atoms, respectively.

(2) Comparison between Model a and Model b. The experimental magnetic coupling constants and those calculated by methods 1 and 2 and the spin populations on Cu1 and Cu2 atoms of models a, b, c, and d by method 1 are listed in Table 2. The *J* values calculated by both methods have the same trend as the experimental ones, although the *J* values by method 2 are closer to experimental data.

The errors of *J* values between the calculated and the experimental results arise mainly because of the methods employed here and the modeling of experimental structures. In addition, the intermolecular interaction and the influence of counterions on magnetic coupling are also not considered. The higher systematical symmetry in the models, compared with the corresponding experimental compounds, usually enhances the antiferromagnetic coupling between magnetic centers.

It can be seen from Table 2 that the *J* value (absolute value) of model a is smaller than that of model b. In contrast, Ruiz et al.[11] have investigated the case of oxygen-bridged Cu(II) binuclear complexes with H atoms and $-CH_3$ groups bonding to the bridging O atoms and found that the *J* value of the former is smaller than that of the latter. The different trends are essentially due to the completely different structure of the bridging ligand in the two cases in which one is a single bridging oxygen atom and the other is an extended bridging group. The sum of the spin populations on Cu(II) ions (absolute values) in model b is smaller than that in model a, supporting the obtained magnetic behavior, because less spin population on Cu(II) ions corresponds to stronger delocalization of the unpaired electrons between Cu(II) ions and leads to stronger coupling interaction.

(3) Comparison of Models b, c, and d. As shown in Table 2, the magnetic coupling constants (absolute values) decrease from model b via c to d, having the same trend as that of the corresponding experimental compounds.[30] This indicates that the magnetic coupling interaction decreases with the terminal ligands out of the plane. The magnetic orbitals of the metal ions in model b favor overlapping because of its coplanar structure. Compared with model b, the extent of the overlapping of the magnetic orbitals in models c and d decreases because of the out-of-plane of the terminal ligands. The magnetic coupling interaction of model c is stronger than that of model d because the terminal ligands in model c have a smaller extent of out-of-plane compared with the case of model d. This variation of *J* values is also confirmed by the variation of the

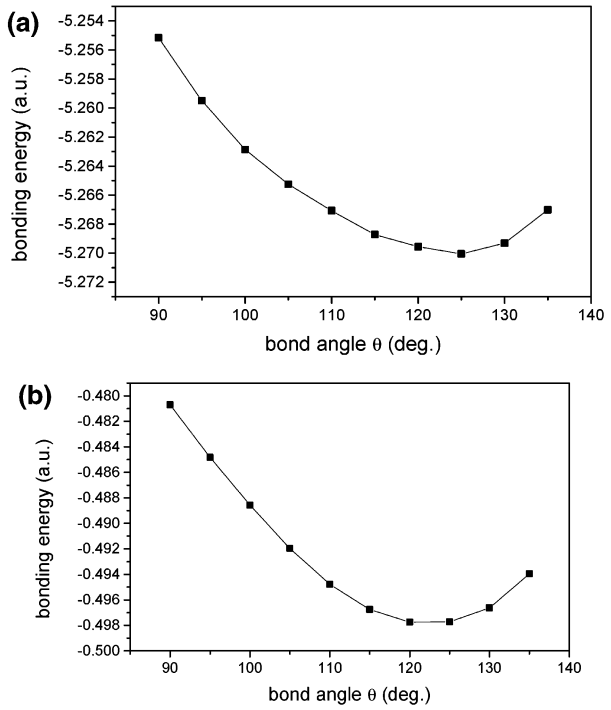

Figure 2. Molecular bonding energy as a function of bond angle θ: (a) calculated by method 1; (b) calculated by method 2.

spin population on Cu1 and Cu2 atoms (Table 2), which increases from models b to d. The increasing spin populations on Cu1 and Cu2 atoms indicate the decreasing delocalization of the unpaired electrons between Cu(II) ions and result in weakening coupling interaction from models b to d.

(4) Investigation of Magnetostructural Correlation. As mentioned above, models c and d are derived from the corresponding experimental compounds. The bond angle θ (θ = N13−Cu1−O6 = N11−Cu1−O6) in model d is larger than that in model c, and the magnetic coupling interaction (absolute value) for model d is weaker than that for model c, which implies that the decrease of bond angle θ may enhance the magnetic coupling interaction. On the basis of the calculated and the experimental results, the bond angle θ is selected to investigate the magnetostructural correlation, although there are many other bond angles that can modify exchange coupling considerably. The strategy is made as follows: let the bond angle θ in model d increase from 90° to 135° with a increment of 5°, under the condition of keeping the three bonds O6−Cu1, N11−Cu1, and N13−Cu1 in one plane. This means that the coordination geometry around Cu1 atom changes gradually from a square pyramid to a trigonal bipyramid with the increase of the bond angle θ. The bonding energy of molecule as a function of bond angle is shown in Figure 2. The relationships $J \approx \theta$, $J \approx \rho$, $J \approx (\epsilon_1 - \epsilon_2)^2$, and $J \approx (\rho_T^2 - \rho_{BS}^2)$ are schematized in Figures 3−6, where ρ_T and ρ_{BS} represent the spin population of triplet and singlet states on Cu atoms, respectively. For the comparison with Figure 3, the relationship between $(\epsilon_1 - \epsilon_2)^2$ and bond angle θ is schematized in Figure 7.

The relationships such as $E \approx \theta$, $J \approx \theta$, and $(\rho_T^2 - \rho_{BS}^2) \approx \theta$ are calculated by both methods. It can be seen from Figures 2, 3, and 6 that each relationship obtained by both the methods has similar trend. Other relationships are mainly obtained by method 1.

Figure 2 indicates that the bonding energy decreases with the increase of the bond angle θ from 90° to 125° and then increases from 130° to 135° or more, namely, a reversion of molecular bonding energy occurs with the bond angle θ larger

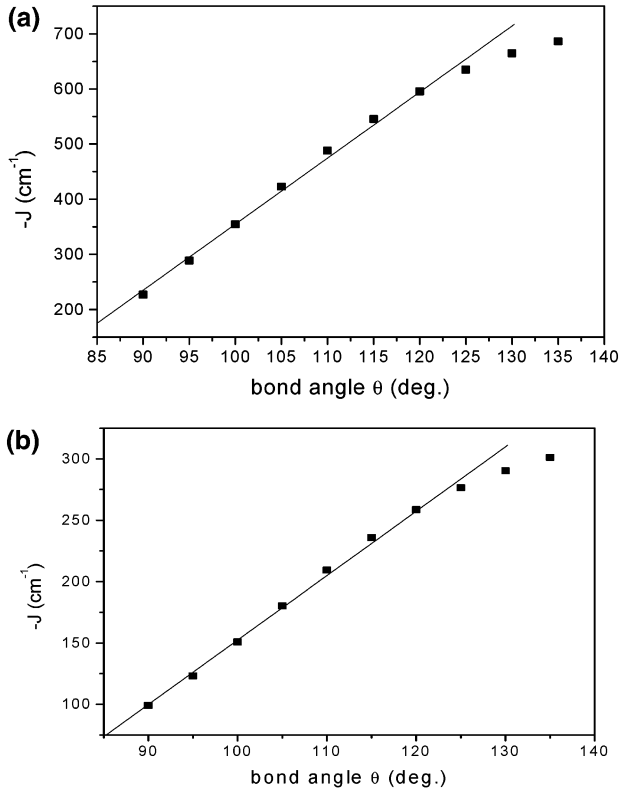

Figure 3. Relationship between the magnetic coupling constant J and the bond angle θ: (a) calculated by method 1; (b) calculated by method 2.

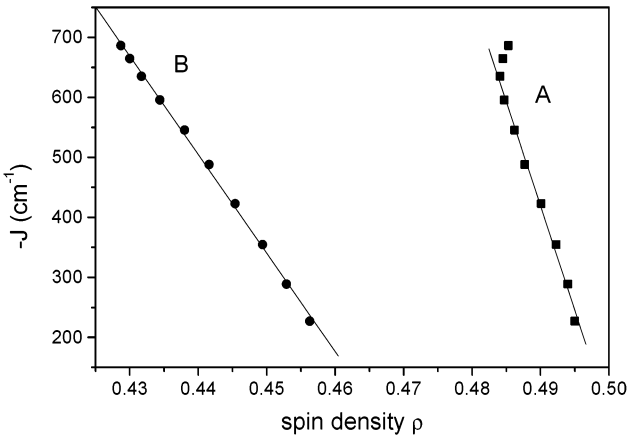

Figure 4. Magnetic coupling constant J as a function of the spin population ρ on Cu1 atom (straight line A) and on Cu2 atom (straight line B). The straight line A is fitted in the bond angle range from 90° to 125°.

than about 125°. This may be explained through the steric hindrance among the three bonds O6−Cu1, N11−Cu1, and N13−Cu1. The steric hindrance decreases as the angle θ increases from 90° to 125°, leading to the decreases of the bonding energy. However, the steric hindrance between the bond N11−Cu1 and N13−Cu1 will be reinforced remarkably with θ larger than 125°, leading to the increases of the bonding energy. Figure 3 shows that the magnetic coupling constant J increases with the decrease of the bond angle θ. There is an approximately linear relationship between J and θ in the angle range from 90° to 125°. The two points in Figure 3 corresponding to θ = 130° and 135° deviate from the straight line.

This fact can be explained through the schematic representation of orbitals. Figure 8 shows the schematic representation of orbitals of model d where the d orbital on Cu2 atom is

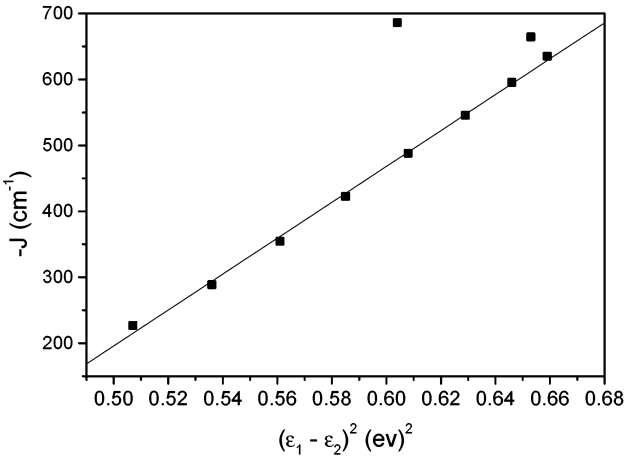

Figure 5. Magnetic coupling constant J as a function of $(\epsilon_1 - \epsilon_2)^2$. The straight line is fitted in the bond angle range from 90° to 125°.

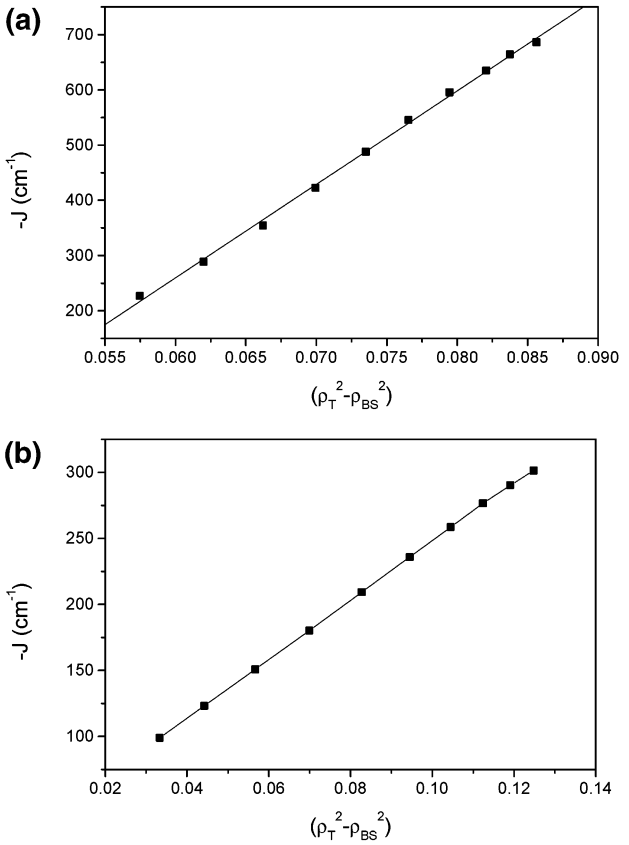

Figure 6. Magnetic coupling constant J as a function of $(\rho_T^2 - \rho_{BS}^2)$ for Cu1 atom: (a) calculated by method 1; (b) calculated by method 2.

perpendicular to that on Cu1 atom. Because of the poor match between both d orbitals, the resulting magnetic exchange coupling is small. Upon the increase of the bond angle θ, the two bonds Cu1−N11 and Cu−N13 are no longer perpendicular to the d orbital on Cu2 atom and approach gradually to the basal plane of the model. The component of d orbital on Cu1 atom will reduce accordingly. So the magnetic orbitals on both magnetic centers match to an increasing extent, leading to the increasing exchange coupling interaction. Although the final two points deviate from the straight line in Figure 3, their coupling interaction still shows an increasing trend. So it can be drawn from above that the key factor controlling the magnitude of magnetic coupling interaction is the symmetry of magnetic orbitals mainly localized on the magnetic centers.

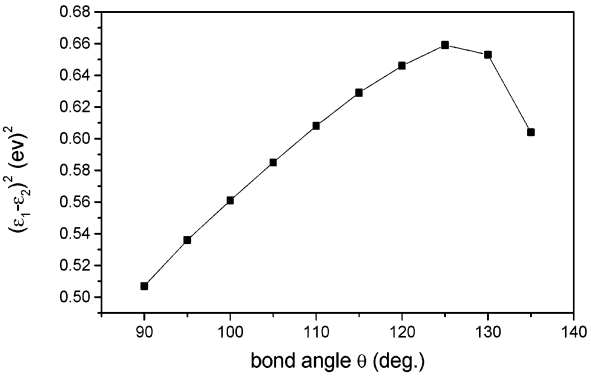

Figure 7. $(\epsilon_1 - \epsilon_2)^2$ as a function of bond angle θ.

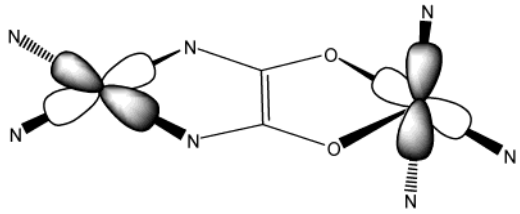

Figure 8. Schematic representation of d orbitals of model d on magnetic centers.

In summary, whether for some symmetrical or for some unsymmetrical binuclear systems, the magnetic coupling constant J is linearly related to the spin populations on magnetic centers with a limited variation of structural parameters. For some symmetrical systems, the linear relationship between J and spin population ρ on magnetic centers has been reported elsewhere with the variation of some structural parameters. This relationship has also been investigated here for the unsymmetrical Cu(II) binuclear complexes. There are two lines in Figure 4 for the relationships between the magnetic coupling constant J and the spin populations on Cu1 and Cu2 atoms, respectively, because the two copper atoms have different coordination environments. It can be seen that the magnetic coupling constant J (absolute value) increases with the reduction of spin populations on the Cu2 atom. With the exception of the two points corresponding to $\theta = 130°$ and 135°, this relationship also occurs on Cu1 atom. Figure 4 shows that there is a good linear relationship between the J value and the spin population on Cu2 atom in the full range $\theta = 90°-135°$, while a linear relationship between the J value and the spin population on Cu1 atom appears except the final two points corresponding to $\theta = 130°$ and 135°. As known, the reinforcement of antiferromagnetic interaction implies the increase of delocalization of the unpaired electrons on magnetic centers toward bridging groups and accordingly the decrease of the spin population on magnetic centers. If the antiferromagnetic interaction is very weak, the unpaired electrons would mainly localize on magnetic centers, leading to large spin population on magnetic centers. So it is understandable to have such trends between J and spin population ρ in Figure 4. Additionally, the spin populations on Cu2 atom keep a better linear relationship to J than those on Cu1 atom. This is due to the changes of θ associated directly with Cu1 atom rather than Cu2 atom. The strengthening of the steric hindrance between the bond N13−Cu1 and N11−Cu1, when $\theta \geq 125°$, mainly has much effect on Cu1 atom. So the spin population on Cu1 is remarkably influenced by the strong steric hindrance, resulting in the deviation of the final two points from the straight line. Because the steric hindrance has not much effect on Cu2 atom, the relationship between J and the spin population ρ on Cu2 atom still keeps a good linear relationship.

The relationship between J and $(\epsilon_1 - \epsilon_2)^2$ is schematized in Figure 5. As indicated by eq 2, there is a linear relationship between J and $(\epsilon_1 - \epsilon_2)^2$ in the bond angle range from 90° to 125°, but there is a deviation from the relationship with the last two points. The obtained straight line indicates that the two-electron integrals K_{ab}, J_{aa}, and J_{bb} are almost unchangeable under the condition that the bonding energy decreases gradually with the bond angle from 90° to 125°. However, these two-electron integrals would have relatively large changes when the bonding energy increases with the bond angle from 130° to 135° or more. So the J values with $\theta > 125°$ no longer keep the same linear relationship to $(\epsilon_1 - \epsilon_2)^2$ as in the range $\theta = 90°-125°$. Because of the increase of the steric hindrance between the bond N13−Cu1 and N11−Cu1 with θ larger than 125°, the molecule becomes more remarkably unstable. Probably, the reason for this discrepancy is the presence of more than two "magnetic" orbitals in such cases that may make the choice of two orbital energies inappropriate to calculate the square of the gap. Throughout Figures 2−5, the common feature is found that the deviation from the linear relationships for J with the parameters mentioned above appears when the bonding energy has a transition from decreasing to increasing.

It can be seen by comparing Figure 2 with Figure 3 that the bonding energy has a reversion with θ more than 125°, while J values vary smoothly with bond angle θ whether more or less than 125°. This indicates that the bonding energy is not a key factor affecting magnetic coupling constant J. It is also found from Figures 3 and 7 that the graphs in both of the figures are similar in the bond angle range from 90° to 125° and obviously different beyond this angle range. So the magnetic coupling constant J can be replaced by $(\epsilon_1 - \epsilon_2)^2$ in describing the magnetostructural correlation in the bond angle range from 90° to 125°, which simplifies the description of magnetostructural correlation by only calculating the energies of the two highest singly occupied molecular orbitals in triplet state, ϵ_1 and ϵ_2.

It should be noted that another parameter $(\rho_T^2 - \rho_{BS}^2)$ is found in this paper showing a linear relationship to J values in the full angle range from 90° to 135°, as shown in Figure 6. Compared with Figure 5, the deviation from the linear relationship is avoided in Figure 6. So the parameter $(\rho_T^2 - \rho_{BS}^2)$ may be more suitable than $(\epsilon_1 - \epsilon_2)^2$ in describing the linear relationship to the magnetic coupling constant J. This can be interpreted theoretically as follows.

The magnetic coupling constant J is proportional to the overlap integral S_{ab}^2,

$$J \propto S_{ab}^{\ 2} \tag{6}$$

The relationship between S_{ab}^2 and $(\rho_T^2 - \rho_{BS}^2)$ has been obtained,[32]

$$S_{ab}^{\ 2} \approx \rho_T^{\ 2} - \rho_{BS}^{\ 2} \tag{7}$$

So

$$J \propto \rho_T^{\ 2} - \rho_{BS}^{\ 2} \tag{8}$$

$(\rho_T^2 - \rho_{BS}^2)$ may be a valuable parameter in this regard and may be extended to other Cu(II) binuclear transition metal systems for the study of magnetostructural correlation. Although in some cases the difference of the spin population gives negative values that will correspond to an imaginary value for the overlap, at least such difference is appropriate for the system studied here and some other systems.[7,10]

It is noteworthy that the relationship between J and $(\rho_T^2 - \rho_{BS}^2)$ is obtained from symmetrical systems. However, Cu(II)−Cu(II) binuclear systems studied in this work are unsymmetrical. Calculated results show that J and $(\rho_T^2 - \rho_{BS}^2)$ still keep a fairly good linear relationship, which implies that the unsymmetry for this system has no larger influence on this relationship. It is found by carefully comparing straight line C with straight line D that the linear regression coefficient of C is smaller than that of D because the variation of structures occurs mainly on Cu1 atom rather than on Cu2 atom. On the basis of the above analysis, we may predict that even for some unsymmetrical binuclear systems, one can approximately describe the magnetic constant J using $(\rho_T^2 - \rho_{BS}^2)$.

Conclusions

The unsymmetrical Cu(II) binuclear complexes bridged by $[C_2O_2(NH)_2]^{2-}$ are studied using broken symmetry approach combined with density functional theory. Different groups bonding to the N atoms of the bridging network $[C_2O_2(NH)_2]^{2-}$ lead to different magnetic coupling interaction. Both the calculated and experimental J values have identical variation trends. The magnetic coupling interaction decreases with the transition of the coordination environments of Cu1 atom in these compounds with the terminal ligands out of the plane because this transition makes the magnetic orbitals unfavorable to overlap. The coupling constant J, as a function of the spin population on Cu1 atom, which has a five-coordinated environment, or $(\epsilon_1 - \epsilon_2)^2$ corresponds to a linear relationship when the bonding energy E decreases with the bond angle θ from 90° to 125° and deviates from the linear relationship when the bonding energy E increases with the bond angle θ more than 125°. Another parameter $(\rho_T^2 - \rho_{BS}^2)$ is found to have a linear relationship to J whether the bonding energy decreases or increases. So the parameter might be more appropriate than $(\epsilon_1 - \epsilon_2)^2$ in the description of the linear relationship to J values.

Acknowledgment. The authors are grateful to Zhida Chen (Beijing University) and Jian Li (Texas Biotechnology Corporation) for their help. This work has been carried out with the financial support of National Science Foundation of China (Grant 20133020).

References and Notes

(1) Kahn, O. *Molecular Magnetism*; VCH: New York, 1993.
(2) Ferlay, S.; Mallsah, T.; Ouahes, R.; Veillet P.; Verdaguer, M. *Nature* **1995,** *378*, 701.
(3) Solomon, E. L.; Brunold, T. C.; Davis, M. Z.; Kemsley, J. N.; Lee, S.-K.; Lehnert, N.; Skulan, A. J.; Yang Y. S.; Zhou, J. *Chem. Rev.* **2000**, *100*, 235.
(4) Holm, R. H. *Pure Appl. Chem.* **1995**, *67*, 217.
(5) Caballol, R.; Castell, O.; Illas, F.; Moreira, I.; De, P. R.; Malrieu, J. P. *J. Phys. Chem. A* **1997**, *101*, 7860.
(6) Cabrero, J.; Ren Amor, N.; de Graaf, C.; Illas, F.; Caballol, R. *J. Phys. Chem. A* **2000**, *104*, 9983.
(7) Hu, H.; Zhang, D.; Chen Z.; Liu, C. *Chem. Phys. Lett.* **2000**, *329*, 255.
(8) Ruiz, E.; Alemany, P.; Alvarez, S.; Cano, J. *Inorg. Chem.* **1997**, *36*, 3683.
(9) Ruiz, E.; Alemany, P.; Alvarez S.; Cano, J. *J. Am. Chem. Soc.* **1997**, *119*, 1297.
(10) Hu, H.; Liu, Y.; Zheng, D.; Liu, C. *J. Mol. Struct. (THEOCHEM)* **2001**, *546*, 73.
(11) Ruiz, E.; Alvarez, S.; Alemany, P. *Chem. Commun.* **1998**, 2767.
(12) Blanchet-Boiteux, C.; Mouesca, J.-M. *J. Phys. Chem. A* **2000**, *104*, 2091.
(13) Ruiz, E.; Cano, J.; Alvarez, S.; Alemany, P. *J. Comput. Chem.* **1999**, *20*, 1669.
(14) Ruiz, E.; Cano, J.; Alvarez, S.; Alemany, P. *J. Am. Chem. Soc.* **1998**, *120*, 11122.

(15) Adamo, C.; Barone, V.; Bencini, A.; Totti, F.; Ciofini, I. *Inorg. Chem.* **1999**, *38*, 1996.
(16) Cano, J.; Alemany, P.; Alvarez, S.; Ruiz, E.; Verdaguer, M. *Chem.—Eur. J.* **1998**, *4*, 476.
(17) Cano, J.; Ruiz, E.; Alemany, P.; Lloret, F.; Alvarez, S. *J. Chem. Soc., Dalton Trans.* **1999**, 1669.
(18) Cano, J.; Rodriguez-Fortea, A.; Alemany, P.; Alvarez, S.; Ruiz, E. *Chem.—Eur. J.* **2000**, *6*, 327.
(19) de Biani, F.; Ruiz, E.; Cano, J.; Novoa, J.; Alvarez, S. *Inorg. Chem.* **2000**, *39*, 3221.
(20) Rodriguez-Fortea, A.; Alemany, P.; Alvarez, S.; Ruiz, E. *Chem.—Eur. J.* **2001**, *7*, 627.
(21) Rodriguez-Fortea, A.; Alemany, P.; Alvarez, S.; Ruiz, E.; Scuiller, A.; Decroix, C.; Marvud, V.; Vaissermann, J.; Verdaguer, M.; Rosenman, I.; Julve, M. *Inorg. Chem.* **2001**, *40*, 5868.
(22) Noodleman, L. *J. Chem. Phys.* **1981**, *74*, 5737.
(23) Hay, P. J.; Thibeault, J. C.; Hoffmann, R. *J. Am. Chem. Soc.* **1975**, *97*, 4884.
(24) Noodleman, L.; Case, D. A.; Aizman, A. *J. Am. Chem. Soc.* **1988**, *110*, 1001.
(25) Mouesca, J. M.; Chen, J. L.; Noodleman, L.; Bashford, D.; Case, D. A. *J. Am. Chem. Soc.* **1994**, *116*, 11898.
(26) Gutsev, G. L.; Ziegler, T. *J. Phys. Chem.* **1991**, *95*, 7220.
(27) Vosko, S. H.; Wilk, L.; Nusair, M. *Can. Phys.* **1980**, *58*, 1200.
(28) Becke, A. D. *Phys. Rev. A* **1998**, *38*, 3098.
(29) Perdew, J. P. *Phys. Rev. B* **1986**, *33*, 8822.
(30) Journaux, Y.; Sletten, J.; Kahn, O. **1985**, *24*, 4063.
(31) Noodleman, L.; Norman, J. G., Jr. *J. Chem. Phys.* **1979**, *70*, 4903.
(32) Ruiz, E.; Cano, J.; Alvarez, S.; Alemany, P. *J. Comput. Chem.* **1999**, *20*, 1391.